Time-Domain Analysis of Excited Subsonic Jet Noise

by

Martin Kearney-Fischer, Aniruddha Sinha, and Mo Samimy

reprinted from

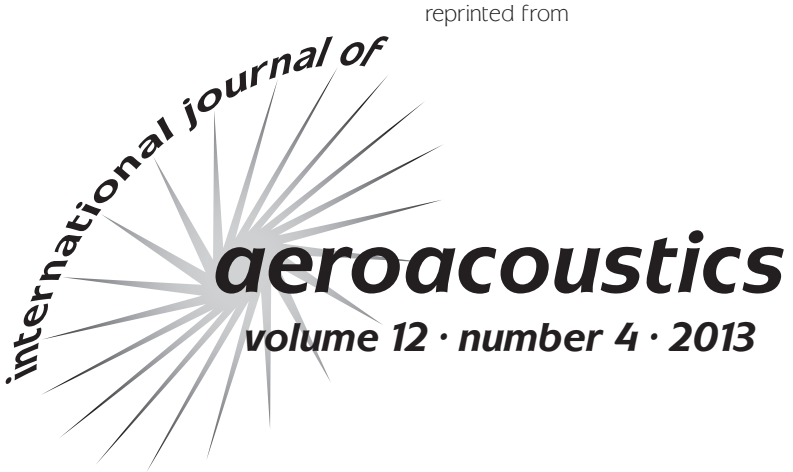

published by MULTI-SCIENCE PUBLISHING CO. LTD.,
5 Wates Way, Brentwood, Essex, CM15 9TB UK
E-MAIL: mscience@globalnet.co.uk
WEBSITE: www.multi-science.co.uk

International Journal of aeroacoustics volume 12 · number 4 · 2013 – pages 387 – 422

Time-Domain Analysis of Excited Subsonic Jet Noise

Martin Kearney-Fischer,* Aniruddha Sinha,† and Mo Samimy‡

Gas Dynamics and Turbulence Laboratory 2300 West Case Rd., Ohio State University, Columbus, OH, 43235, USA

Received: May 2. 2013; Revised Aug. 29, 2013; Accepted Sept. 15, 2013

ABSTRACT

Building on previous work showing that far-field jet noise has significant intermittent aspects and the statistical analysis of those intermittent aspects, the present work applies the same analysis techniques to an excited jet. Using an experimental database covering several operating conditions [jet Mach number (M_j = 0.9), nozzle diameter (D = 2.54 cm), and jet stagnation temperature ratios (TTR = 1.0 – 2.5)] and a wide array of excitation parameters (azimuthal mode m_F = 0, 1, & 3 and Strouhal number St_{DF} = 0.09 – 3.0), these events are extracted from the far-field noise signals measured in an anechoic chamber. This database is analyzed to determine how the noise event characteristics are altered by excitation. The relationship between the noise events and the flow-field dynamics of the excited jet are discussed. Analysis of the excited jet reveals the existence of a resonance condition. When excited at the resonance condition, large noise amplification occurs – this is associated with nearly every large-scale structure producing a noise event. Conversely, noise reduction occurs when only one noise event occurs per several large-scale structures. The impact of the azimuthal extent of large-scale structures is explored using a wave-packet model to provide support to the discussion of azimuthal mode radiation efficiency. The results indicate that there is a competition for flow energy among neighboring structures that dictates if and how their dynamics will produce noise that radiates to the far-field. Furthermore, the azimuthal model supports the conclusion that higher modes are less efficient radiators. These various factors provide support for the conclusion that the mechanism of noise reduction involves inducing the jet into a condition where the naturally occurring structures are suppressed by excited structures which are less efficient radiators (i.e. higher azimuthal modes at frequencies where neighboring structures destructively compete for flow energy).

1. INTRODUCTION

Six decades of research have not yet revealed a clear understanding of jet noise [1, 2]. While there have been advances in empirically based models [3, 4] and theoretical analysis [5, 6] of jet noise, the essential features of jet noise are still debated. Without a complete description of the essential features of jet noise, understanding of their sources is clearly impeded.

*Currently at Lockheed Martin Aeronautics.

†Currently Postdoctoral Scholar at California Institute of Technology.

‡Nordholt Professor of Mechanical and Aerospace Engineering. Corresponding Author: samimy.1@osu.edu

Two methods of experimental data analysis have dominated the study of jet aeroacoustics: Fourier spectrum analysis and correlation analysis. These two tools provide researchers with a wealth of information and insight, but with certain restrictions. In most spectral analysis, phase information is discarded making it impossible to link particular aspects of the frequency domain back to segments of the signal in time. Correlation analysis shows links between two signals in time, but only if their trends are sufficiently similar.

These two tools are likely overlooking some of the fundamental aspects of jet noise. Recently, some researchers have started using wavelet transforms to obtain a more complete picture of the noise signal (see §2.2). The basic theme of these works is the supposition that acoustically subsonic jet noise (at least in the radiation to aft angles) is made up of intermittent bursts as opposed to continuous variations. If this assertion is presumed to be accurate, understanding this kind of signal requires a different analysis methodology than has been prevalent in the literature.

In recent works from the Gas Dynamics and Turbulence Laboratory (GDTL) of the Ohio State University, Kearney-Fischer et al. [7-9] used a peak identification technique to isolate intermittent bursts in the noise signals from a wide range of polar angles and jet operating conditions. In this context, a noise event is defined as a portion of the signal that exceeded 1.5 times the root mean square far-field pressure fluctuations, $1.5p_{RMS}$. The previous study of an unexcited jet [9] showed that these bursts (hereafter referred to as "noise events") are the dominant feature of the noise signals at low polar angles relative to the jet downstream axis. Additionally, an in depth statistical analysis of these events was conducted revealing trends relevant to the understanding of jet noise. Some of the key findings are: noise events are statistically independent phenomena and noise event characteristics in unheated jets scale with diameter and not jet acoustic Mach number. The purpose of the present work is to apply this previously developed analysis methodology and understanding to excited jets to see how the statistical quantities are altered when the instability dynamics of the jet are controlled.

2. BACKGROUND

It is generally accepted that jet noise is produced by the interaction and development, as well as the disintegration of turbulent structures [10]. Beyond this point, the description of noise production processes gets quite complicated. In subsonic jets, the evolution, interaction, and disintegration of flow structures produce what is known as mixing noise. Theoretical approaches to the problem have provided insights, but an elegant description of a source and its relationship to the noise produced has not been obtained. Theoretical analyses, beginning with the pioneering work of Lighthill [1], struggle to untangle the non-linear nature of the governing equations into a form that clearly identifies a source.

2.1 Flow Control

Experiments on controlling the development of the jet plume have been going on for almost as long as jets have been in use. Previous studies of jet flow control include both passive (geometrical modifications of the nozzle such as chevrons, lobed nozzles, etc.)

[11-16] and active (can be turned off to eliminate performance penalties when unneeded) control techniques [17-23]. Jets have several instabilities which have been well researched in low-speed and low Reynolds number jets [17-27]. These instabilities are: the jet initial shear layer instability, the jet column or jet preferred mode instability, instability related to significant density gradients in the jet, and, in the case of an axisymmetric jet, the azimuthal component of instability.

GDTL has developed a class of plasma actuators, called Localized Arc Filament Plasma Actuators (LAFPAs), that can provide excitation signals of high amplitude and high frequency for high-speed and high Reynolds number flow control [28,29]. These actuators work by exciting the instabilities that exist in the jet. GDTL has used these actuators for noise and flow control studies in both subsonic and supersonic jets [30-38].

It should be noted that the structures in jets excited by this active control method have a primarily span-wise extent – in this context, span-wise means that the vortex axis is aligned with the azimuthal axis of the jet. Previous works [34] have shown that excitation with these actuators produces regular structures over a wide range of frequencies and that the induced structure spacing is dictated by the excitation frequency. While not discussed here in detail, various data reduction methods such as the jet width, turbulent kinetic energy, phase locking, proper orthogonal decomposition, and vortex identification techniques have been used to characterize the behavior of the excited large-scale structures. Based on these analyses, several conclusions were reached about the excited large-scale structure characteristics.

1. The largest structures are created by exciting the jet near the jet column natural Strouhal number ($St_{DF} = f_F D/U_j \approx 0.3$). U_j is the jet exit velocity and the subscript "F" denotes an excitation parameter.
2. The largest structures are created by exciting azimuthal mode ±1, mode 1, and then mode 0 in decreasing order of size. Higher order structures (e.g. $m_F = 3$) are smaller still.
3. Individual structures created by excitation are detectable from arbitrarily low excitation Strouhal numbers to $St_{DF} \approx 1.5$. Each firing of an actuator within this frequency range generates a structure.
4. Depending on the azimuthal mode of the excitation, the structures created by the individual actuators merge into different shapes (e.g. mode 0 merges into a ring, mode 1 into a helix, etc.). The rate at which this merger occurs depends on the forcing azimuthal mode and also the excitation frequency.
5. Structures excited near $St_{DF} \approx 0.7$ initially grow more rapidly than those at $St_{DF} \approx 0.3$ and then convect for a few jet diameters (about 2-4) without significant development. This is particularly true of mode 0 and this behavior is accentuated at elevated temperatures. Exciting structures at these (and nearby) frequencies, especially with high order azimuthal modes (e.g. $m_F = 3$) reduces the amount of noise produced.

2.2 Temporally Localized Signal Analysis

While spectral analysis is the standard tool of jet noise research, there is some precedent in the literature for jet noise analysis assuming a fundamentally intermittent signals [39-45]. A common tool used in these works is wavelet analysis – the underlying principle of which is that the signals under examination cannot be adequately described by a set of periodic waves.

In the previous works at GDTL [39,46], the assumption of intermittence provided a basis for a source localization method. Noise events were defined as spikes rising above a specified threshold in the time domain. Simultaneous flow-visualizations using a MHz-rate imaging system showed that these events are associated with dynamically significant behavior of the large-scale structures. Guj et al. [43] used a similar kind of conditional averaging of the flow-field to determine that bursts of noise were related to dynamically significant fluctuations of the large-scale structures. They also called attention to the limitations of Fourier analysis to illuminate this kind of phenomenon.

Cavalieri et al. [47] looked at the Direct Numerical Simulations (DNS) of an uncontrolled and an optimally noise-controlled two-dimensional mixing layer computed by Wei and Freund [48]. They showed that the optimally controlled case accomplishes noise reduction by suppressing certain intermittent peaks in the signal – highlighting the need to include intermittency in sound prediction schemes. Cavalieri et al. [41] discussed a wave-packet model in which the envelope function varies in both space and time. This analysis, which follows the idea originally suggested by Kastner et al. [49], shows that a high amplitude event (i.e. a spike in the far-field pressure) can be produced when the wave-packet is truncated by fluctuations in the envelope. Grassucci et al. [40] used a wavelet domain filter to separate near-field pressure fluctuations into intermittent and non-intermittent signals. They then related the intermittent signal to velocity fluctuations in the jet using Linear Stochastic Estimation. While this work is preliminary, their initial results are promising. Grizzi et al. [50] used wavelet transforms to separate the acoustic and hydrodynamic fluctuations in near-field pressure data. The group at the University of Poitiers [42,51,52] have started using wavelet transforms and filtering in the wavelet domain to isolate these intermittent events for study. This analysis used a 4th order Paul wavelet to decompose the signals with a continuous wavelet transform. Results to date have mainly focused on the relationship of the resulting directivity patterns to wave-packet models for jet noise. A group at Syracuse University [45, 53] used wavelet filtering and correlation on both near and far-field to determine how the near-field events are related to the far-field events. Some of their work is still preliminary, but warrants mentioning as a significant attempt to trace the intermittent aspects of jet noise back toward their sources.

These works show that jet noise does indeed contain intermittent events and that these events play a significant role in the overall acoustic picture of the jet. The results to date, however, are quite limited in their description of these intermittent events. Issues such as the importance of these events to the total signal spectra, many aspects of the nature of these events (lifetimes, frequency of occurrence, etc.), and exact relationship of these events to the flow-field dynamics remain to be determined.

2.3 Noise Event Definition and Identification Method

The two essential features of the noise event definition used in this work are: 1) primary noise sources in a mixing noise dominated jet (i.e. acoustically subsonic), at least those that radiate to aft angles measured relative to the jet downstream axis, are intermittent "events" with periods of relative silence in between; and 2) a noise event is defined as a contiguous set of points whose peak amplitude exceeds $\pm 1.5 p_{RMS}$. The validity of this noise event definition has been established on a large dataset of unforced subsonic jets in a previous work from GDTL [9]. A detailed description of the noise event extraction method is given in [9], so only a concise description is provided here. It should be noted that the analysis algorithm in the present work is identical to that applied in the previous one. None of the parameters of the algorithm were adjusted in any way. For any identified event, its amplitude (A_i), width (δt_i – defined as the full width at half maximum), and location in time (T_i) are extracted. For the exclusive purpose of calculating the spectrum of a signal containing only these events, each event is reconstructed using the above three parameters and a Mexican hat function. Events are assumed to be independent and so the reconstructed signal is a superposition of the individual events. It should be noted that event location and width are determined to single sample accuracy of the discretely sampled acoustic signal and are not interpolated to a higher precision. One consequence of this data extraction method is that the minimum event width allowed is three samples. Any subsequent analysis of these quantities will also be quantized at single sample accuracy.

2.4 Unexcited Database Results

The following are some of the key conclusions reached by the analysis of the unexcited jet noise database documented in [9].

1. The far-field acoustic signal radiating to the aft polar angles can be well represented by intermittent bursts of noise.
2. Using a model with three parameters in the acoustic signal (peak amplitude, event width, and the time between events), the following are educed from the analysis.
   (a) The distribution of peak amplitudes obeys a universal normal distribution across all polar angles and operating conditions once scaled by p_{RMS} of the original signal. The normal distribution ($\sigma = 1.2$) is close to the unit normal but slightly skewed toward larger amplitudes.
   (b) The distribution of event widths (looking only at the aft polar angles) obeys a universal gamma distribution ($\ell \approx 6.0$ & $\xi \approx 0.17$, where ℓ and ξ are the gamma distribution shape and scale parameters, respectively) for all cases at a given polar angle once scaled by the mean event width ($\overline{\delta t}$). There are small variations in the gamma parameters with polar angle, but the distributions are reasonably well described by a single universal distribution for all angles below about $\phi = 50^\circ$. The fact that a gamma distribution accurately describes the event widths implies that the width of one event has no correlation to the width of other events.
   (c) The distribution of the event intermittence has the same characteristics as the event width once scaled by the mean intermittence ($\overline{\Delta T}$). This implies that

the occurrence of one event is not correlated to the occurrence of preceding or subsequent events.

(d) There is a consistent relationship between the mean event width and the mean intermittence ($\overline{\delta t} = 0.128\overline{\Delta T}$). This implies a strong link between the governing dynamics controlling these two quantities.

3. Based on these observations, the entire signal for noise radiated to the aft angles can be reasonably well predicted in a statistical sense with knowledge of three quantities (p_{RMS}, $\overline{\delta t}$, and $\overline{\Delta T}$) along with the $\sigma = 1.2$ normal distribution and the gamma distribution ($\ell \approx 6.0$ & $\xi \approx 0.17$). It is actually possible to eliminate one or other of the mean quantities if the relationship from point 2(d) is used.

3. EXPERIMENTAL SETUP

All of the experiments on excited jets are conducted in the anechoic chamber at GDTL within the Aeronautical and Astronautical Research Laboratories (AARL) at Ohio State University.

3.1 Test Facility

The jet simulation facility at GDTL is of blow-down type. The compressed air, supplied with three 5-stage reciprocating compressors, is filtered, dried, and stored in two cylindrical tanks with a volume of 43 m^3 and pressure up to 16 MPa. The compressed air is passed through a storage heater at a set temperature to heat up the air to the desired temperature and supplied to the stagnation chamber of the jet facility with an axisymmetric nozzle. The air is discharged horizontally through the nozzle into an anechoic chamber and then through an exhaust system to the outdoors (Fig. 1a). The anechoic chamber in these experiments has an open volume of about 25 m^3 and is rendered anechoic down to about 250 Hz using fiberglass wedges. The chamber validation is documented in Kerechanin et al. [54]. The nozzle for the experiments reported in this work is stainless steel, axisymmetric with an exit diameter of $D = 2.54$ cm (1 in.).

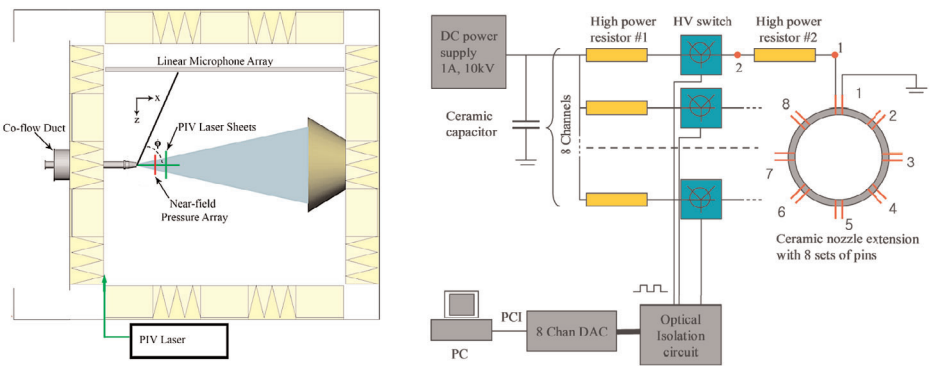

(a) Jet facility and anechoic chamber.

(b) LAFPA circuit and nozzle schematic.

Figure 1: Experimental setup for the GDTL facility.

3.2 Plasma Actuators

As discussed in §2.1, GDTL has developed a type of flow control actuator known as the LAFPA. The LAFPA circuit and a schematic of the actuator layout on the nozzle are shown in Fig. 1b. Each actuator consists of a pair of pin electrodes held in place using a nozzle extension. The electrodes are distributed around the nozzle perimeter, approximately 1 mm upstream of the nozzle extension exit plane. The nozzle extension is made of boron nitride and tungsten wires of 1 mm diameter are used for electrodes. Measured center-to-center, the spacing between a pair of electrodes for each actuator is 4 mm, and the distance between the neighboring electrodes of two adjacent actuators is 6 mm. With this arrangement, eight actuators are uniformly distributed around the nozzle extension so that the azimuthal spacing between two adjacent actuators is 45°. More information on the plasma actuators can be found in previous publications from GDTL [28, 29].

3.3 Acoustic Measurements

The diagnostic tool used in the work discussed here is a far-field acoustic system. The far-field Sound Pressure Level (SPL) is measured using 1/4 inch Bruel & Kjaer 4939 microphones. Acoustic data are collected using a linear microphone array with ten microphones measuring angles of ϕ = 25°, 30°, 35°, 40°, 45°, 50°, 60°, 70°, 80°, and 90° relative to the jet downstream axis. The array axis is parallel to the jet axis and the microphones are mounted normal to the array axis. Testing confirmed that the only observable changes in spectra acquired with the microphones mounted as described, as opposed to radial (also referred to as normal) incidence, are due to the sensitivity of the microphones. The resulting radial distances from the nozzle exit to the microphones range from 49D (at 90°) to 116D (at 25°). The acoustic signal from each microphone is band-pass filtered from 20 Hz to 100 kHz, amplified by one of three four-channel Bruel & Kjaer Nexus 2690 conditioning amplifiers, and acquired using National Instruments PXI-6133 A/D boards and LabView software. The microphones are calibrated using a 114 dB, 1 kHz sine wave, and the frequency response of the microphones is flat up to 80 kHz with the microphone grid cover removed. Sample signals are collected at 200 kHz with 8192 data points per segment producing a spectral resolution of 24.4 Hz.

Table 1: Experimental operating conditions.

D (cm)	M_j	TTR	$Re_D \times 10^{-5}$	M_a	ETR
2.54	0.9	1.0	6.12	0.83	0.86
		1.5	3.65	1.02	1.29
		2.0	2.57	1.18	1.72
		2.5	1.98	1.32	2.15

Table 2: Excitation parameters.

Azimuthal Mode (m_F)	Excitation Strouhal Number (St_{DF})
0, 1, 3	0.09 – 3.0

An average SPL spectrum is obtained from the mean square of 100 short-time spectra. More information on the microphone hardware and spectral analysis techniques is available in [37].

3.4 Experimental Parameters

Since the goal of this work is to explore mixing noise from subsonic jets, a jet with a Mach number of 0.9 at different Total Temperature Ratios (TTR) was chosen for study. Some quantities relevant to the experimental operating conditions – the Reynolds number (Re_D), acoustic Mach number (M_a), and Exit Temperature Ratio (ETR) – are computed in Table 1. While some of these cases aren't acoustically subsonic in the strictest sense ($M_a < 1$), a previous work has shown that these jets do not display any strong supersonic noise characteristics [55]. Based on that result, it was determined that the data from these experiments was acceptable for the analysis undertaken in the present work.

The excitation parameters used on these jets are shown in Table 2 – the subscript "F" signifies forced and is used to denote an excitation quantity for several variables. Previous works [37] showed that the changes in the acoustic field of the jet were minimal outside this range of excitation frequencies. The axisymmetric mode ($m_F = 0$) and the 1st order helical mode ($m_F = 1$) are canonical choices for excitation based on the literature discussed in §2.1. Additionally, Suzuki and Colonius [56] have shown that azimuthal $m_F = 0$ mode growth in an unexcited jet is significantly more enhanced by heating of the jet than that of modes 1 and 2. This same phenomenon has also been reported by Hall and Glauser [57] and previous work by GDTL [33] discusses some experimental results of this behavior with respect to LAFPAs. Previous work showed that $m_F = 3$ (the highest mode accessible by the 8 actuators used) produced the greatest reductions in the far-field noise levels [37]. The excitation parameter space (Table 2) is based on these observations. A spectral analysis of this data has been published in a previous work [37] and additional discussion of the data can be found there.

4. EXCITED JET ANALYSIS

In this section, the impact of excitation on the noise events is analyzed using the GDTL database. This is accomplished by first performing a spectral analysis of the data to determine how the jet responds to excitation using the traditional tool. The reason for this is to identify excitation cases that produce the greatest changes in the SPL and/or the Overall Sound Pressure Level (OASPL) and then to relate those changes to changes in the noise event characteristics.

4.1 Spectral Analysis

In the previous works from GDTL on the acoustic field of an excited jet, it has been common to remove narrowband tones associated with excitation to focus on the changes in the broadband spectral shape [37,58]. This was done for two reasons: 1) there is potentially a component of the signal acquired by the DAQ system that is electronic noise associated with the plasma based excitation, and 2) the actuators emit a compression wave that is detectable at the microphones (referred to as actuator self-

noise). It has been determined in previous works that these contaminants were relatively weak in most cases, but it will always be difficult to tell what portions of the narrowband tones originate in the flow-field. Given the obvious complications associated with attempting to extract the time domain signature of the electronic noise and compression waves associated with excitation without impacting the noise produced by the jet, it will be assumed that the validity of the acquired signal must be evaluated as a whole and no attempt to condition the data will be made.

The experimental data used in this analysis is well documented in a previous GDTL publication [37] so only selected aspects of the spectral analysis are discussed in this paper.

4.1.1 Changes in OASPL

The changes in OASPL for the angular domain as a function of excitation Strouhal number are discussed to determine how the excitation parameters impact the noise. ΔOASPL ($OASPL_{excited} - OASPL_{baseline}$) curves for $\phi = 30^\circ$ for the various parameters are shown in Fig. 2 – much more comprehensive plots are in the previous work [37]. In the unheated cases, the reductions observed at the aft angles are somewhat consistent with the general amplification over most of the angles (not shown) and excitation Strouhal numbers. The lack of distinction between excitation azimuthal modes, however, indicates that the energy of the narrowband tones is playing a significant role in the measured OASPL. Furthermore, the variation in the energy of the narrowband tones as a function of the excitation frequency makes it difficult to discern any trends in the data. The narrowband spectra show that the broadband jet noise is being altered, but the complex nature of these ΔOASPL maps makes interpretation almost impossible.

The results at the elevated temperatures show that the trends become much clearer as the temperature increases. In mode 0, there is a strong amplification region at the low excitation frequencies and aft angles. In contrast, modes 1 and 3 have no such strong amplification region. The results clearly show that by proper selection of St_{DF} and excitation azimuthal mode, one can obtain some amount of noise reduction across all measured radiation angles for temperature ratios TTR $\geq$ 2.0. A more detailed examination of the ΔOASPL maps yields the following observations.

1. The far-field noise signature of the unheated jet seems to contain a significant amount of actuator self-noise that obscures trends in the OASPL. This diminishes as the jet is heated because the jet gets louder.
2. In the elevated temperatures, $m_F = 0$ develops a strong increase in OASPL at the aft angles ($\phi < 50^\circ$) for excitation Strouhal numbers near the jet column natural frequency ($St_D \approx 0.3$). Close inspection reveals that the greatest increase occurs at the excitation frequency of $St_{DF} = 0.18$. This suggests that exciting the jet with mode 0 at that frequency reinforces the naturally occurring event phenomena. Examination of the narrowband spectra indicates that this additional energy is contained in the narrowband tones. Since this behavior is not observed in the other modes, it is concluded that this is indeed a flow-field response as opposed to actuator electronic noise or self-noise. The cause for this is likely the confluence of two separate mechanisms: a disproportionate increase in $m = 0$ energy content

in unexcited heated jets and superdirective radiation. The latter will be discussed more in subsequent sections.

3. While difficult to determine from the lower temperatures alone, the complete picture indicates that $m_F = 3$ produces the largest decreases in the OASPL and that these decreases occur at the lowest angles measured (ϕ = 25° & 30°).
4. The excitation Strouhal number that removes the most energy at the aft angles decreases with increasing temperature and is different for the different azimuthal modes. The mode 0 minimum occurs near $St_{DF} \approx 1.3$, while modes 1 and 3 occur at $St_{DF} \approx 0.5$. Additionally, the precise amount of far-field acoustic energy that can be removed by excitation increases with increasing temperature.
5. While smaller amounts of reduction at all angles is achievable, the larger amounts of reduction at the aft angles are generally accompanied by amplification at the higher angles. Additionally, uniform reduction at all angles is not likely to be a desired characteristic since the energy radiating to different polar angles varies quite significantly (i.e. -3dB at 30° is a larger removal of energy than -3dB at 90°).

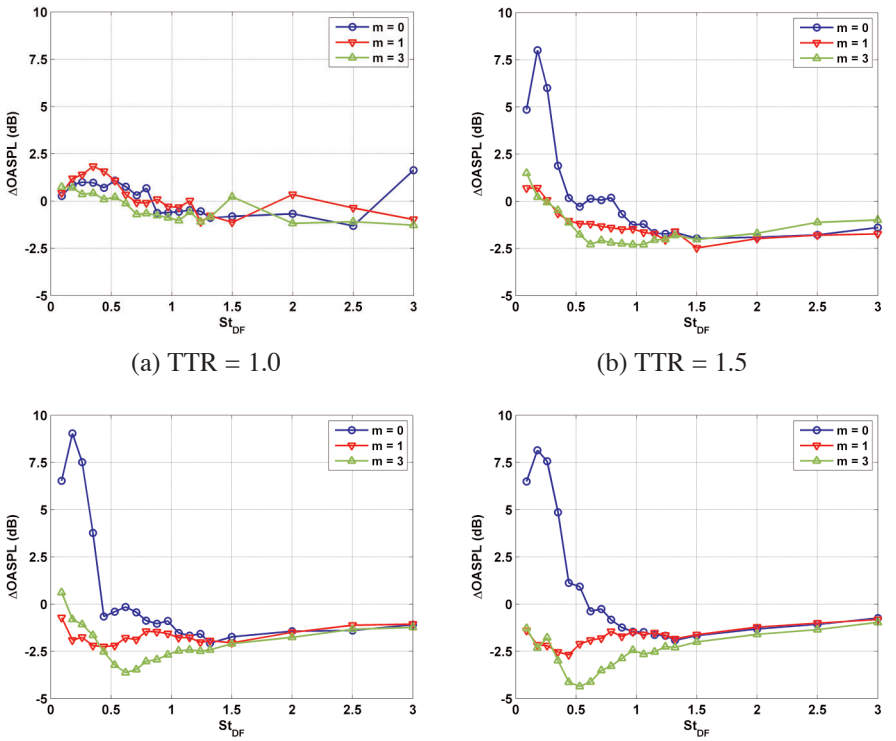

(a) TTR = 1.0 (b) TTR = 1.5

(c) TTR = 2.0 (d) TTR = 2.5

Figure 2: ΔOASPL plots for ϕ = 30°.

It has been observed that the amount of energy found in the $m = 0$ flow-field mode of unexcited jets grows disproportionately faster than the other modes with increasing jet temperature [56, 57]. Reinforcing this natural mechanism with excitation would likely produce axisymmetric flow-field structures that have significantly increased spatial and temporal coherence – a conclusion that is supported by a previous work using particle image velocimetry [33]. Another way to say this is that the flow becomes more receptive to $m = 0$ development. It is also generally accepted (see [56, 63]) that the axisymmetric mode is the most efficient radiator of sound in the peak radiation direction (i.e. aft angles) [60]. The concept of superdirective radiation in jet noise, originally discussed by Crighton and Huerre [59], describes the radiation pattern from a noise source that can't be decomposed into a finite series of multipoles. In an unexcited jet, there are a wide range of oscillation frequencies with randomized phases that would result in energy being distributed in time and frequency space. If one frequency becomes dominant (say through the combination of disproportionate increases in mode receptivity and excitation), the energy of the radiation should be concentrated in both time and frequency space. The directive aspects of the ΔOASPL maps and the narrowband spectra (not shown) support this assertion. The observation of this phenomenon only in the axisymmetric mode suggests that the spatial coherence of the structures is an important factor in the radiating efficiency of this mechanism.

4.1.2 Events-Only Comparison

Using the same process described for the unexcited jet data analyzed in [9], the spectra of the events-only signals are computed and compared to the data spectra. The unexcited results are very similar to the results in [9] that were determined from a different dataset; which confirms the generality of the results as well as the procedure.

The spectral behaviors in the excited jet are qualitatively similar to the unexcited jet results [9] in most cases across the range of temperature and excitation parameters. The one area in which the reconstructed spectrum behavior is significantly different is in the elevated temperatures at aft angles and specifically when exciting the axisymmetric mode ($m_F = 0$) at low excitation Strouhal numbers ($St_{DF} = 0.1 – 0.5$). In these cases, the spectral peak frequency is in reasonably good agreement, but the spectral amplitude is significantly over-predicted. Examining the spectra at these parameters reveals that this behavior occurs in the region of the ΔOASPL maps where strong amplification was observed. This over-prediction is another indicator that something different is happening in the acoustic field when the jet is excited axisymmetrically near the jet column natural frequency ($St_D = 0.3$) in these heated cases. This behavior occurs only for the axisymmetric mode; it is completely absent in both the $m_F = 1$ and $m_F = 3$ cases.

Looking at the time-domain version of the signal (not shown), the reason for the reconstruction behavior is readily apparent. When excited with these parameters in the elevated temperatures, the noise radiated to aft angles becomes highly periodic (with a period matching the excitation frequency) containing long chains of high-amplitude events. This apparent resonance condition results in over-prediction of the event peaks because the model function exaggerates the resonance – the superposition of neighboring events leads to excess amplitude.

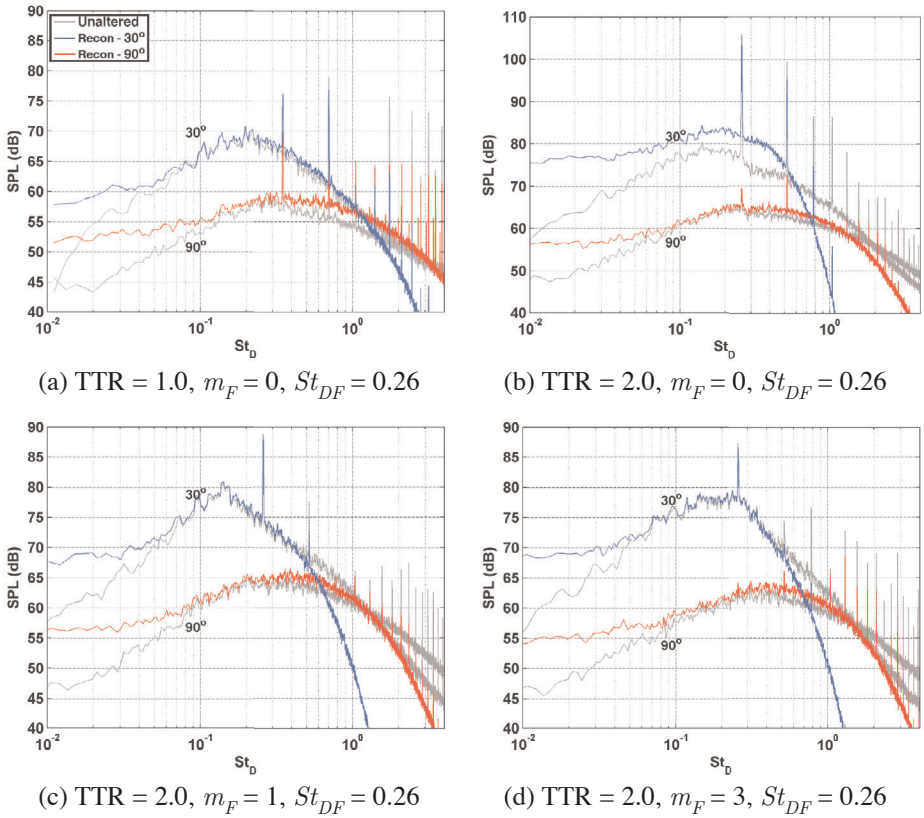

(a) TTR = 1.0, $m_F = 0$, $St_{DF} = 0.26$

(b) TTR = 2.0, $m_F = 0$, $St_{DF} = 0.26$

(c) TTR = 2.0, $m_F = 1$, $St_{DF} = 0.26$

(d) TTR = 2.0, $m_F = 3$, $St_{DF} = 0.26$

Figure 3: Example spectra showing the over-prediction phenomenon. The colored spectra are reconstructions and the gray spectra are unaltered data.

4.2 Statistical Analysis

Based on the spectral analysis of the excited jet, it is concluded that the excited jet dynamics are fundamentally similar to the unexcited jet [9] with the few exceptions already discussed. The most relevant conclusion is that the statistical analysis of the events can focus on the aft angles (30° is used) without missing important information. Additionally, the unexcited cases within the GDTL database do not need to be explored in great detail except for comparison purposes to excited cases. The unexcited jet results show that the statistics of event width and intermittence have very similar behaviors. As discussed in [9], the event width and intermittence statistics are both well described by the gamma distribution; the two variables are even described by gamma distributions with very similar parameters ($\ell \approx 6.0$ & $\xi \approx 0.17$, where ℓ and ξ are the gamma distribution shape and scale parameters, respectively). Additionally, the previous results [9] showed that there is a strong statistical correlation between the mean event width ($\overline{\delta t}$) and the mean intermittence ($\overline{\Delta T}$); the ratio of these quantities for 30° averaged over all

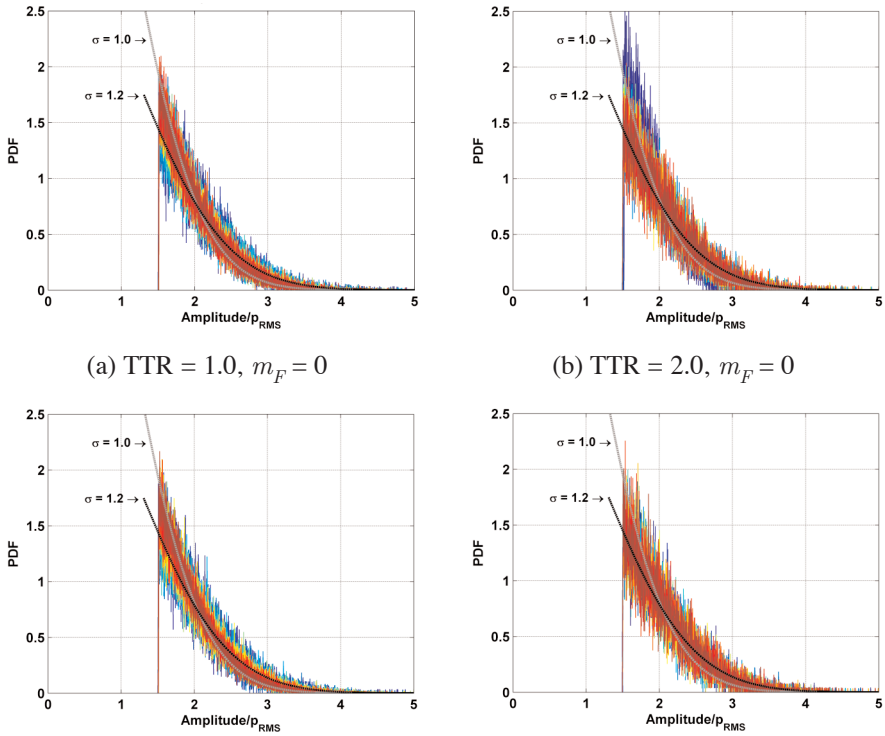

(a) TTR = 1.0, $m_F = 0$ (b) TTR = 2.0, $m_F = 0$

(c) TTR = 1.0, $m_F = 1$ (d) TTR = 2.0, $m_F = 1$

Figure 4: PDF of peak amplitudes for all excitation frequencies at $\phi = 30°$. Higher frequencies are in red and lower frequencies in blue.

cases was $\overline{\delta t}/\overline{\Delta T} = 0.128 \pm 0.002$ and was shown to be a good scaling for all the polar angles, diameters, and operating conditions examined in [9]. Therefore, the intermittence is discussed in detail (given its relevance to the resonance phenomenon discussed above) along with the mean width and mean intermittence.

4.2.1 Amplitude Distributions

The Probability Density Functions (PDFs) for the peak amplitudes of extracted events at 30° are shown in Fig. 4 for all excitation frequencies at azimuthal modes 0 & 1 and temperature ratios of 1.0 and 2.0. The distributions, for the most part, are very similar to the unexcited jet [9]; which is to say that the distributions are well described by the normal distribution with a standard deviation of $\sigma = 1.2$. As discussed in [9], the unexcited event amplitude distributions skew away from the unit normal because the peaks only contain part of the information about points above the $1.5p_{RMS}$ threshold. There are two notable differences in the excited jet results. In the unheated jet, it can be seen that the higher frequencies (the redder curves) are skewing toward the unit normal

distribution for both modes. This variation is relatively slight and, given the likelihood that the data has a large amount of actuator self-noise as already discussed (§4.1), it is not likely that it is a meaningful variation. At the elevated temperature cases (TTR = 2.0) shown in Fig. 4, the departure from the baseline distribution (i.e. departure from $\sigma = 1.2$ curve) is associated with the strong increases in the OASPL. In mode 0, the low excitation frequencies (blues) have an amplitude distribution close to the unit normal while mode 1 has no such trend. This change is likely associated with a basic change in the nature of the typical event created by exciting with these parameters. The typical event in these highly excited cases, however, is different from the typical event in most other cases; these cases are characterized by periodic high-amplitude oscillations. The peaky characteristics of these events mean that the peak amplitude is more representative of the data above the threshold so it recovers a distribution close to the unit normal-the distribution of the total signal (see [9]). While not shown, the other polar angles, temperatures, and azimuthal modes have amplitude distribution characteristics consistent with a combined interpretation of the unexcited results and the range of excitation frequencies and polar angles where the strong amplification occurs.

4.2.2 Intermittence Distributions

The amplitude distributions indicate that, in most cases, the excited jet statistics behave similarly to the unexcited jet. Therefore, a few examples of the intermittence distributions are shown in Fig. 5 to illustrate the different characteristics that appear in the intermittence distributions. Note that these distributions are normalized by their respective means, consistent with previous analysis [9]. In each of these figures, the unexcited intermittence distribution (baseline) is shown as a black or gray line and excitation periods are indicated by downward pointing triangles.

In the unheated jet at $\phi = 30^\circ$ excited with mode 0 (Fig. 5a), the deviation at low excitation frequencies is due to narrowband spikes that are multiples of the excitation period. The distribution at these conditions retains the same basic shape as the baseline. At the higher excitation frequencies, the intermittence distribution is being significantly altered. Very strong spikes are visible (multiples of the excitation period) and these cause the shape of the distribution to flatten.

Looking at the same polar angle and excitation mode but at an elevated temperature (Fig. 5b) reveals just how radically the distribution is being altered by low frequency excitation. For low excitation frequencies near the jet column natural frequency ($St_D \approx 0.3$), the distribution is dominated by a spike at the excitation period with weaker spikes at multiples of the fundamental period. The occurrence of events with these few periodicities is so high that the remaining portions of the distribution have negligibly small probabilities. For the same conditions at large excitation frequencies, however, the distribution is indistinguishable from baseline. To look at directivity, the intermittence distributions at $\phi = 60^\circ$ are shown (Fig. 5c) for the same temperature and excitation parameters as in Fig. 5b. It is clear that the distribution deviates only slightly from the baseline due to excitation. The strongest deviation in the 60° distributions is a narrowband spike associated with the excitation period when the excitation frequency is near the jet column natural frequency – this supports the presence of a strong

resonance phenomenon with strong radiation directivity. Finally, to examine the excitation mode response, the intermittence distributions for mode 3 (Fig. 5d) are shown for the same polar angle and temperature as (Fig. 5b) with one exception. In (Fig. 5d), the distributions are plotted for all the excitation frequencies. It is clear that exciting this mode does not create strong deviations from the baseline distribution. There are a few narrowband spikes at the fundamental periods for a few of the lower excitation frequencies, but the distribution shape is essentially unchanged.

In the cases where the distribution is not being significantly altered by excitation (i.e. baseline-like cases), it can be seen that the intermittence distributions are well described by the gamma distribution. As discussed in relation to the unexcited jet [9], the gamma distribution arises from Poisson processes. In a Poisson process, the occurrences of events of interest are independent from one another, and so these occurrences (e.g. wait times) are distributed randomly about some mean. It is therefore expected that a quantity like the intermittence would be described by the gamma distribution.

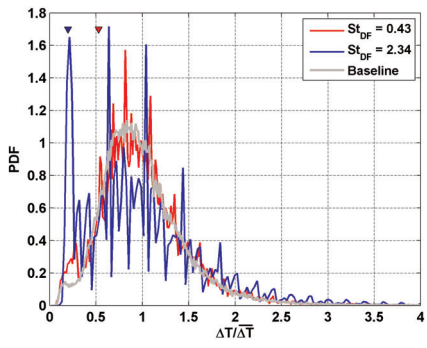

(a) TTR = 1.0, $\phi = 30^\circ$, $m_F = 0$

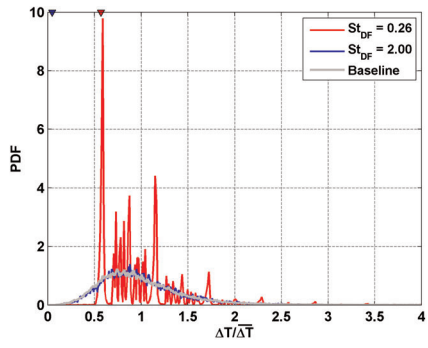

(b) TTR = 2.0, $\phi = 30^\circ$, $m_F = 0$

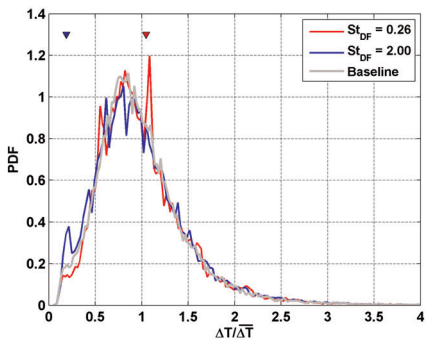

(c) TTR = 2.0, $\phi = 60^\circ$, $m_F = 0$

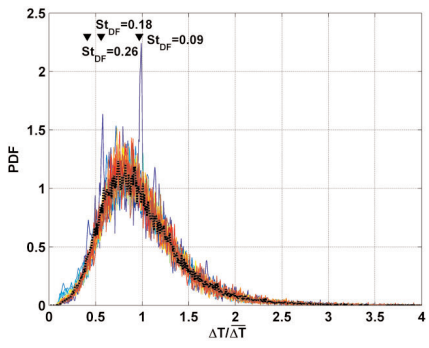

(d) TTR = 2.0, $\phi = 30^\circ$, $m_F = 3$ for baseline and 19 excitation frequencies.

Figure 5: Intermittence distributions normalized by their respective means for the excited jet.

To get an overall picture of the intermittence distribution behaviors without presenting an unwieldy number of plots, the following metric is used to describe how much a particular case deviates from the baseline distribution. The distributions are normalized by their respective means as done in [9]. The best fit gamma distribution for the unexcited data (baseline) is determined for a given operating condition and polar angle. The RMS error of a particular distribution with respect to the baseline best fit gamma distribution is computed. Finally, this RMS error is normalized by the RMS error of the baseline distribution with respect to its own best fit gamma distribution. This quantity is referred to as the "gamma deviation." In this way, quantities significantly greater than one indicate a distribution that is a meaningful departure from the baseline while removing the expected changes in the distribution. From the results discussed in [9], the intermittence distribution is dependent on the jet diameter and temperature, but is only significantly dependent on velocity at elevated temperatures.

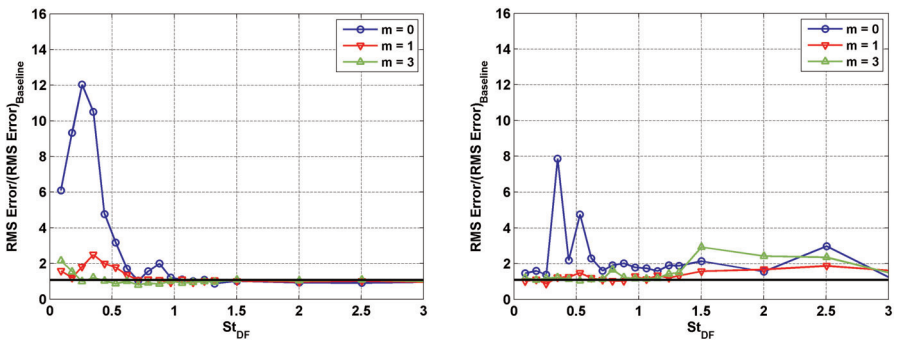

(a) $\phi = 30^\circ$ (b) $\phi = 60^\circ$

Figure 6: Gamma deviations for TTR = 2.0 at $\phi = 30^\circ$, & 60°. The black line marks the baseline result.

The gamma deviation for a couple of polar angles are shown in Fig. 6 for all the forcing cases under study in the TTR = 2.0 jet. Modes 1 and 3 have very little deviation except for a small amount at the sideline angles for high excitation frequencies. Mode 0, in contrast, shows a very strong localized deviation that correlates very well with the excitation frequency and directivity characteristics of the large OASPL increase already discussed (§4.1). The other polar angles and temperatures (not shown) have behaviors and trends consistent with the results shown, except for the self-noise issues observed in the unheated jet. The TTR = 1.5 case behaves like the TTR = 2.0 case implying that the diminution of the self-noise problem occurs somewhere between TTR = 1.0 and TTR = 1.5. In the unheated case (not shown), there is substantial deviation from the gamma distribution regardless of excitation frequency, azimuthal mode, or polar angle. The indiscriminate deviation with respect to excitation frequency in the unheated case supports the previous conclusion that actuator self-noise is a prominent feature at this operating condition.

It can be seen that the gamma deviation is indeed a good descriptor of changes in the distribution shape. Additionally, the intermittence results add support to the conclusion that the jet at elevated temperatures is generating strong superdirective radiation when excited with the axisymmetric mode near the jet column natural frequency.

4.2.3 Mean Width and Intermittence

Based on the unexcited jet analysis [9], the mean width ($\overline{\delta t}$) and intermittence ($\overline{\Delta T}$) are parameters governing the changes in the jet noise signal characteristics. Additionally, a strong link between these two quantities was observed ($\overline{\delta t}/\overline{\Delta T} = 0.128$) [9]. That same scaling is applied to the data in this section to see if the behavior is preserved under excitation and to minimize the number of needed figures.

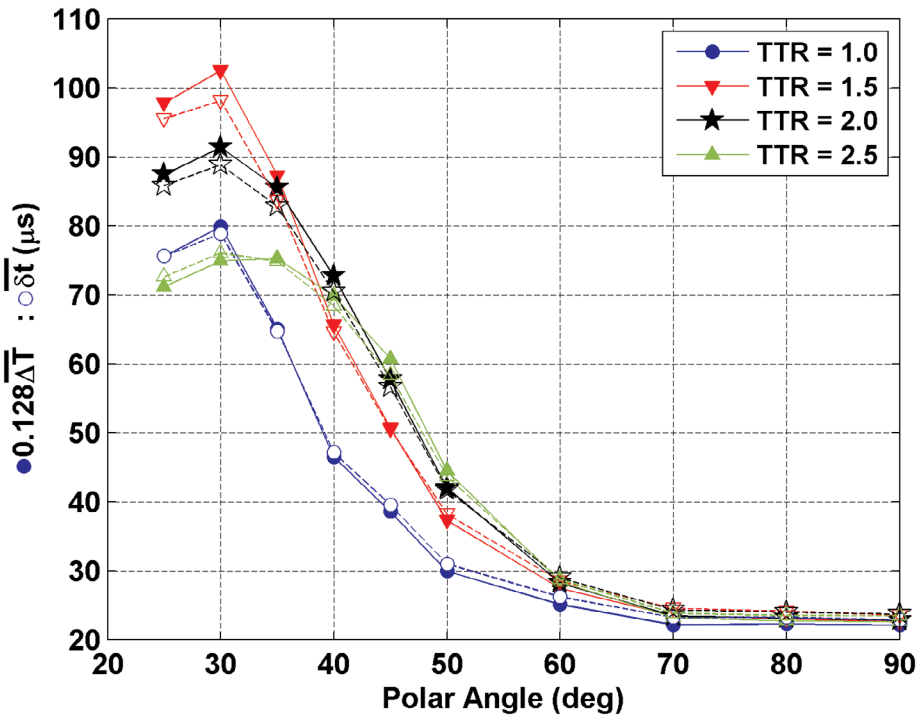

Figure 7: Mean width and intermittence for the baseline jet data from GDTL.

The unexcited (baseline) mean quantities for the GDTL data are shown in Fig. 7. Comparing these data to the unexcited database of the previous work [9], there are some similarities and some differences. The experiments conducted at GDTL utilize a thick-lipped nozzle whereas the NASA data [9] used thin-lipped nozzles so some differences should be expected; particularly in sideline and upstream radiation directions. It should first be noted that the scaling factor of 0.128 between the mean event width and intermittence is consistently a good scaling in the GDTL data, as it was for the NASA

data. Looking at the unheated case (TTR = 1.0) – for which a nearly direct comparison exists in Case 4 of the unexcited work [9] – the distributions are very similar. The mean width at $\phi = 30^\circ$ is nearly identical between the two databases; as is the trend to the sideline angles. The mean width at $\phi = 90^\circ$ is slightly lower in the GDTL facility, but it is unlikely that the discrepancy is significant. The only discrepancy of note in the unheated case is the behavior at $\phi = 25^\circ$. In the unexcited data [9], the event width continues increasing with decreasing polar angle. The GDTL data, however, changes direction below $\phi = 30^\circ$. This is most likely a facility dependence in the GDTL facility created by the location of the $\phi = 25^\circ$ microphone within the anechoic chamber. The $\phi = 25^\circ$ microphone is located in a corner of the anechoic chamber in relatively close proximity to the walls and the collector – the data in the unexcited work [9], in contrast, has no such proximity issue. It is therefore likely that noise reaching this microphone is being altered by this proximity and discussion of this angle should be minimized. This observation is noteworthy because this issue is not readily apparent from the SPL spectra.

The trend with increasing jet temperature in the GDTL database is a much more complex comparison. The GDTL database holds a fixed Mach number while varying the stagnation temperature ratio whereas the previous work [9] holds the acoustic Mach number constant while varying the exit temperature ratio. One consequence of this is that the GDTL jet becomes acoustically supersonic (as seen in Table 1). Previous work has shown that Mach wave radiation onset should occur in the higher temperatures of the jet currently under discussion [55], but that it should be a relatively weak contribution in terms of the acoustic spectra. Looking at the transition ($\phi = 40^\circ$ to 60°) and sideline angles, the trend with increasing temperature in the GDTL data is similar to the unexcited previous work [9]. The aft angles, however, have a trend (i.e. mean quantities monotonically increase with increasing temperature) that is similar to the previous work for the lower temperatures, but that reverses direction for the two highest temperature ratios. Unless compressibility effects, created by the combined increase in temperature and velocity, are producing changes in the source mechanisms of the mixing noise sources, it is likely that this behavior is indicative of the presence of Mach wave radiation, but that the Mach wave radiation source is too weak to produce any significant changes in the spectral shape. This result dictates that any significant changes in excitation response between TTR = 1.5 & 2.0 or TTR = 2.0 & 2.5 at the aft angles, must be discussed with the possibility of competing noise sources in mind.

The mean width and intermittence for $\phi = 30^\circ$ are shown in Fig. 8 for the four temperature ratios. The excitation period (T_F) is also shown in these figures for context. Looking at the unheated jet first, it can be seen that the scaling of 0.128 is held quite well regardless of excitation parameters at this temperature. Again there is evidence that the data has significant actuator self-noise: the azimuthal modes are indistinguishable and trend consistently downward to smaller and smaller intervals with increasing excitation frequency. It is difficult to say from the data, but it appears that the mean event width is asymptotically approaching the excitation period. Comparing these data to the ΔOASPL data offers very little insight except to confirm the indistinguishable nature of the different azimuthal modes at this temperature.

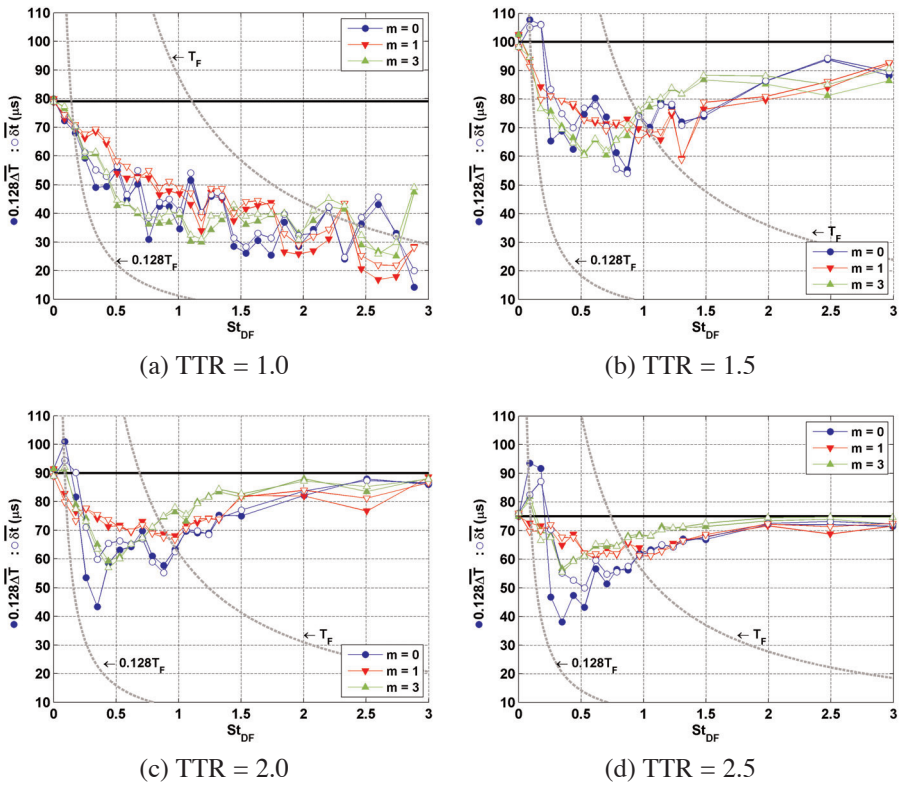

Figure 8: Mean width and intermittence for various temperatures at $\phi = 30^{\circ}$. T_F is the excitation period.

At a temperature ratio of 1.5, the trends in the mean width and intermittence are starkly different from those of the unheated jet. The different azimuthal modes trend down to some minimum and then trend back toward the baseline levels with increasing excitation frequency. This reinforces the idea that the jet is being excited without overwhelming the acoustic field with actuator self-noise. It is also clear in this case that the different azimuthal modes are affecting the mean quantities in different ways.

In mode 0, the mean intermittence closely follows the excitation period for excitation frequencies less than $St_{DF} \approx 0.3$ as might be expected from the previous discussions. Even at the lowest excitation frequencies measured, the noise source dynamics are still so strongly controlled by the excitation that the intermittence increases above the baseline. It should be remembered, however, that the relationship between the intermittence distribution and the mean is strained in these strong response cases (i.e. $m_F = 0$ at elevated temperatures with $St_{DF} \leq 0.6$). When the baseline distribution is obliterated by a strong periodicity, the mode of the distribution will be the best

descriptor. As already discussed (§4.2.2), the mode of the distribution in these strong response cases is exactly the excitation frequency. This explains why the mean intermittence in these cases follows the excitation frequency while not matching it. The amplification of the OASPL peaks (see Fig. 2) at the excitation frequency for which the excited mean intermittence matches the baseline (at an excitation frequency of $St_{DF} \approx 0.2$). This strongly suggests the idea that the excitation frequency is matching a naturally occurring resonance. Another observation of mode 0 excitation is that, for the low frequencies ($St_{DF} < 0.6$), the changes in mean width are smaller than the changes in the intermittence. This suggests that, while the dynamics governing the width and intermittence are strongly related, the behavior of one does not necessarily determine the exact behavior of the other. The changes induced by exciting modes 1 and 3 aren't as dramatic as mode 0. In these modes, there is always good agreement between the width and intermittence. Mode 1 has a gradual trend with a large flat trough – the peak noise reduction (see Fig. 2) occurs somewhere in this local minimum. Mode 3 has a more pronounced minimum with noise reduction peaking at excitation frequencies just larger than the intermittence minimum.

The behavior of the jet in response to excitation frequency and azimuthal mode suggest a process of competition, both in the temporal axis (which is highly correlated with the axial direction) and the azimuthal axis. One of the general results is that significant noise reduction occurs when the excitation period is smaller than the induced mean intermittence, and also larger than the induced mean event width. The maximum noise reduction occurs when the induced mean intermittence period is roughly five times greater than excitation period. Studies of the flow-field (see references discussed in §2.1) have shown that excitation at these frequencies generates a single structure for each pulse of the actuator. If the mean intermittence doesn't match the excitation period, the implication is that only some of the structures are producing noise events. It appears that the noise sources radiating to the aft angles (i.e. large-scale structures) are competing for flow energy. Noise reduction occurs when excitation produces an environment in which this competition limits the amount of energy that any one structure can consume. Conversely, noise amplification occurs when excitation tunes the jet to allow each structure to consume large amounts of energy.

4.3 Summary of Results

As already established in previous publications [31, 34, 37], the plasma actuators are capable of manipulating jet noise. The spectral analysis therein shows that:

1. The reduction/amplification characteristics depend on jet temperature, Mach number, excitation frequency and azimuthal mode, and polar angle.
2. The excitation tone amplitude of $m_F = 0$ at the aft angles ($\phi < 50^\circ$) increases at elevated temperatures for excitation Strouhal numbers near the jet column natural frequency ($St_D \approx 0.3$). Close inspection reveals that the greatest increase occurs at the excitation frequency of $St_{DF} = 0.18$. This suggests that exciting the jet with mode 0 at that frequency reinforces the naturally occurring event periodicity. These changes in the tone amplitude create large changes in the OASPL that occur

only in mode 0. This is highly suggestive of strong superdirective radiation and its prominence at elevated temperatures is likely related to the disproportionate growth of mode 0 energy in the unexcited jet when the temperature is elevated.

3. Actuator self-noise appears to be a significant contribution to the noise signature in the unheated jet, but becomes inconsequential at elevated temperatures because the jet gets louder.
4. While difficult to determine from the lower temperatures alone, the complete picture indicates that $m_F = 3$ produces the largest decreases in the OASPL at aft angles (e.g. $\phi = 30°$).
5. The excitation Strouhal number that removes the most energy at the aft angles decreases with increasing temperature and is different for the different azimuthal modes: the mode 0 minimum occurs near $St_{DF} \approx 1.3$, while modes 1 and 3 have their minima at $St_{DF} \approx 0.5$.
6. Strong reduction at the aft angles is accompanied by amplification at the higher angles. Uniform reduction is achievable when exciting at high frequencies, but the reduction is quantitatively smaller than peak reduction levels. Also, there isn't any well-defined optimum excitation frequency or azimuthal mode for reduction at the high forcing frequencies because the amount of reduction is not significantly frequency dependent at these frequencies.

The statistical analysis based on noise-event identification provides the following additional insights.

1. Actuator self-noise is a problem in the statistical metrics of the unheated jet – reinforcing the conclusion from the spectral analysis.
2. In most cases, the statistical description of the jet noise (i.e. the shape of the PDF) is not being significantly changed by excitation.
3. When excited in the strongly resonant regime (i.e. $m_F = 0$ and $St_{DF} \approx 0.1 – 0.5$ at elevated temperatures), the naturally occurring (i.e. unexcited) statistical distributions of the event intermittence are totally obliterated by a single intermittence interval equal to the forcing period. This suggests that the excitation is achieving a resonance with the natural frequencies of the jet – supported by the fact that the strongest resonance occurs when the induced mean intermittence matches the baseline mean intermittence.
4. The relationship between the mean intermittence ($\overline{\Delta T}$) and width ($\overline{\delta t}$) as determined from the unexcited jet ($\overline{\delta t}/\overline{\Delta T}$ =0.128) is still valid in the excited jet with one exception. In the strongly resonant regime, the mean width is not as strongly affected compared to the mean intermittence. This divergence in the relationship between these two quantities suggests that the mechanisms responsible for these characteristics are linked, but that one does not always dictate the exact nature of the other.
5. The nature of the jet response, both in terms of frequency and azimuthal mode, suggests a process in which noise sources are competing for flow energy. Noise reduction occurs when excitation produces a competitive environment that limits

the amount of energy that any one structure can extract from the mean flow – limiting a structure's ability to produce a noise event. Conversely, noise amplification occurs when excitation tunes the jet to allow each structure to extract large amounts of energy from the mean flow – resulting in large noise events.

5. MEASUREMENTS OF STRUCTURE INTERACTION

The results discussed in §4 highlighted questions about the behavior and interaction of the large-scale structures in the jet (both in terms of the excited jet behavior and also what that infers about the unexcited jet). The two most important observations are the discussion of a resonance condition and how neighboring structure competition for flow energy affects noise production. While there are many questions that could be explored regarding the nature of the structure interaction, the two most critical to this analysis are:

1. What is the impulse response of the jet? The impulse response of the jet is something that has not been well studied in the literature. The explorations of jet or shear layer excitation in the literature usually focus on the response to single frequency excitation and then sweep that frequency [22].
2. Can evidence of competition for flow energy be found and what is the behavior of that competition?

In an effort to address these questions, GDTL recently conducted experiments using excitation and a linear microphone array placed in the hydrodynamic near-field region. A study of the impulse response characteristics of the hydrodynamic near-field, along with frequency sweeps and linear parabolized stability equation analysis, was recently published [61]. This publication covers many aspects of the key characteristics and discussion of the excited flow structures (including the experimental setup), so only a couple relevant aspects are discussed here.

The data presented here was measured at a distance of $3D$ downstream of the nozzle exit and about $2D$ radially. The axisymmetric mode (m_F = 0) was excited with frequencies ranging from very low (250 Hz or St_{DF} = 0.02) to moderate Strouhal numbers (St_{DF} = 1.4). Exciting the jet at very low frequencies is equivalent to exciting the jet with a single pulse because all of the timescales of the jet are very small compared to the excitation period. The jet examined was the same M_j = 0.9, D = 2.54 cm, unheated jet (TTR = 1.0) studied in §4. While it was shown that actuator self-noise was a problem in the acoustic far-field, the amplitude of the hydrodynamic pressure fluctuations is much higher so actuator self-noise is not a significant problem.

As discussed in [61], the experiments show that the jet readily supports the existence of an isolated large-scale structure (i.e. a structure excited by a single actuator pulse). One consequence of this impulse response (shown in Fig. 9b as the black line) nature of the jet is that, for excitation frequencies low enough to keep the structures separated, the energy per unit time should add independently and be directly related to the excitation frequency (see [61] for more discussion of structure superposition). Based on

the impulse response duration of about 0.6 milliseconds, this threshold would correspond to a frequency of about 1.67 kHz (St_D = 0.15). For structure occurrence frequencies higher than this, it is expected that interaction and competition for energy should take place. To get an overview sense of this, the mean square pressure of the phase-averaged signals (averaged over 1000 periods) at various excitation frequencies is calculated and normalized by the jet exit kinetic energy density (Fig. 9a). The unexcited mean square pressure (Baseline) is marked for reference. The line associated with the independent addition of energy, using the impulse response energy as the reference point, is also shown.

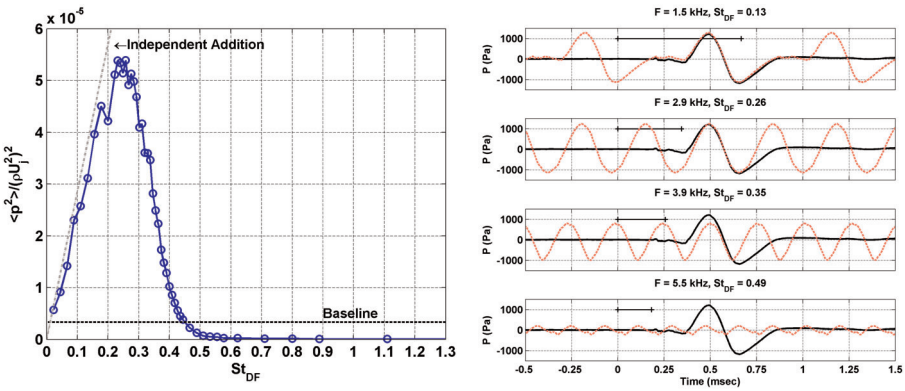

(a) Mean square pressure of the phase-averaged pressure signal for axisymmetric excitation at various frequencies.

(b) Examples of the large-scale structure signature for various excitation frequencies.

Figure 9: Near-field response characteristics.

To assess how the structures are being affected, several examples are shown in Fig. 9b. For each example, the phase-averaged signal is shown along with the impulse response signal and the excitation period is marked by a black bar. The first example (St_{DF} = 0.13) is the highest frequency for which the adjacent impulse responses (including the actuator acoustic wave) don't interact. It can be seen that, at this and any lower excitation frequency, the structures do not interact in an appreciable way. The second example (St_{DF} = 0.26) shows how the structures start interacting when the energy per unit time is maximized. The amplitude of the signal is unchanged from the impulse response, but the adjacent structures are compressing one another slightly resulting in an almost perfectly sinusoidal shape. The next example (St_{DF} = 0.35) shows a case where the interaction of the structures has started to inhibit structure growth. The amplitude is reduced and the structures are increasingly compressed (remember that the time axis of these data are directly related to spatial extent by way of the convective velocity of the structures). In the last example (St_{DF} = 0.49), the inhibition of structure

growth by competition has become quite severe. The expected periodicity is still present, but the amplitude and shape of the structure signature is significantly altered.

These results reveal several important aspects about the large-scale structure behavior and interaction in the jet. As seen in these data, as well as previous experiments using LAFPAs (§2.1), excitation produces one structure per excitation period over a wide range of frequencies. At this point, it could be said that this statement is true over the range $St_{DF} = 0$ to $St_{DF} \approx 1.5$ (the reasoning behind the upper bound is discussed in [38]). The size and energy of a structure (at least for $m = 0$ structures) is only dependent on the frequency for frequencies greater than $St_{DF} \approx 0.15$. For frequencies greater than this threshold, the structures interact, first in a way that increases the energy density (i.e. energy per unit time), but then in a competitive manner that inhibits the ability of the structures to extract energy from the flow. The frequency that results in the greatest energy density ($St_{DF} = 0.25$) is in the same region as the postulated resonance phenomenon discussed in §4. While the numbers don't line up exactly, they are quite close and factors such as temperature have not been taken into account at this point.

Turning these conclusions toward the unexcited jet reveals the following. Structures that are separated by a sufficient distance (i.e. separated by a distance corresponding to frequencies less than $St_D \approx 0.15$) have similar energy per structure, but greater separation equates to less energy per unit time. As the structure spacing approaches resonance ($St_D \approx 0.2$), the maximum energy per unit time is reached. Beyond resonance, the structures compete for energy and drag down the energy per unit time. As long as the energy radiated to the far-field is even loosely related to the energy of the structures (a conclusion supported by all of the other results), this distribution of energy provides an explanation for why the strongest events in the acoustic far-field are associated with a resonance frequency. While additional experiments examining these characteristics as a function of excitation azimuthal mode and temperature should be conducted to further investigate the observed behavior, the current results are quite informative.

6. THE RELATIONSHIP BETWEEN AZIMUTHAL EXTENT AND RADIATION POWER

The analysis of noise events shows that a resonance exists in the jet – evidenced by the large noise amplification that can occur when the jet is excited at a frequency matching the mean intermittence of the unexcited jet. In this case, at least in a statistical sense, every large-scale structure produces a noise event (see Fig. 5b). This analysis also shows that significant noise reduction occurs when only a fraction of the large-scale structures produce noise events. The experimental results support the idea that noise sources are competing for flow energy and that these noise sources are closely related to the large-scale structures. These results can be divided into two areas: a general behavior of competition, and the specific impact of azimuthal extent. Both these areas have been discussed in the preceding sections, but there is some additional insight to be gained by looking at a mathematical analysis of the effect of azimuthal coherence on radiating efficiency.

As already established, the excited jet results show that the azimuthal extent of the structures plays a significant role in the aft-angle noise. One method for exploring this

issue is through a superdirective noise model (i.e. a wave-packet) [59, 63]. In this case, the noise source is modeled as lying on a cylinder whose radius is the same as nozzle radius (R). Using a simple wave-packet model for the axial fluctuations, the noise source term can be written as

$$T_{11}(\mathbf{y},\tau) \propto R\delta(r-R)\exp\left[\mathrm{i}(\omega\tau - ky_1) - y_1^2\lambda^{-2}\right]\sum_{n=-\infty}^{\infty} C_n e^{\mathrm{i}n\theta}, \tag{1}$$

where ($\mathbf{y}$,τ) is the source-field coordinate system ($r,\ \theta,\ y_1,\ \tau$), R is the jet radius, λ is the axial envelope size, and the azimuthal source components are represented by a Fourier series. Using only the T_{11} component of the source tensor is acceptable because this term dominates the solution for radiation to the aft angles as utilized in many other works in the literature (e.g. [41]). While eqn (1) is written in complex form for analytical convenience, only the real part represents the physical solution, so the imaginary part may be discarded where convenient.

The solution to Lighthill's equation using only the T_{11} source term with the far-field assumption in cylindrical coordinates is

$$p(\mathbf{x},t) = \frac{\cos^2\phi}{4\pi|\mathbf{x}|a_\infty^2}\frac{\partial^2}{\partial t^2}\int_{-\infty}^{\infty}\int_0^{2\pi}\int_0^{\infty} T_{11}\left[\mathbf{y}, t-|\mathbf{x}-\mathbf{y}|/a_\infty\right] r dr d\theta dy_1, \tag{2}$$

where ($\mathbf{x}$,t) is the far-field coordinate system ($r_x,\ \theta_x,\ \phi,\ t$) and ϕ is the polar coordinate (i.e. the same microphone angle used previously). Using this assumption, the distance between the source and observer in the far-field in spherical coordinates is approximately

$$|\mathbf{x}-\mathbf{y}| \approx |\mathbf{x}| - y_1\cos\phi - r\cos[\theta-\theta_x]\sin\phi, \tag{3}$$

where θ_x is the azimuthal coordinate in the far-field. Inserting the source term and evaluating the trivial radial integration, the far-field pressure is

$$\begin{aligned} p(\mathbf{x},t) \propto & \frac{R^2\cos^2\phi}{4\pi|\mathbf{x}|a_\infty^2}\frac{\partial^2}{\partial t^2}\exp\left[\mathrm{i}\omega(t-|\mathbf{x}|/a_\infty)\right]\times \\ & \sum_{n=-\infty}^{\infty}\int_{-\infty}^{\infty}\exp\left[\mathrm{i}(\omega\cos\phi/a_\infty - k)y_1 - y_1^2\lambda^{-2}\right] C_n dy_1 \times \\ & e^{\mathrm{i}n\theta_x}\int_0^{2\pi}\exp\left[\mathrm{i}\omega R\cos[\theta-\theta_x]\sin\phi/a_\infty\right] e^{\mathrm{i}n(\theta-\theta_x)} d\theta. \end{aligned} \tag{4}$$

Inspection reveals that the primary difference between eqn (4) and its one-dimensional model equivalent (i.e. line-source model located on the jet centerline, not shown) is the appearance of a factor containing the azimuthal integral – as should be expected. This integral is of the form of Bessel's first integral so it can be evaluated as

$$\Theta_n = 2\pi\mathrm{i}^n J_n\left[\pi St_D M_a\sin\phi\right], \tag{5}$$

where J_n is the nth order Bessel function of the first kind. If ($\pi St_D M_a \sin \phi$) ≈ 0, all $J_n \approx 0$ except for J_0 so only the axisymmetric sources can radiate when the argument of the Bessel function is small unless this factor is offset by the Fourier coefficients – a result noted by Cavalieri et al. [41]. This is mathematical support for the idea that the axisymmetric mode is the most efficient radiator of aft-angle jet noise – at least within the scope of these simple models. Equation (5) also indicates that the axisymmetric mode is the most efficient radiator for low Strouhal numbers regardless of polar angle, but it must be remembered that the polar angle directivity is dictated by other factors in the model. This result provides a possible explanation for the experimental results showing that exciting the axisymmetric mode with low Strouhal numbers results in strong amplification. Since it is possible for the azimuthal Fourier coefficients (C_n) to be functions of t or y_1, the coefficient factor must be left inside the axial integral and time derivatives of eqn (4). If C_n are not functions of t or y_1, the far-field pressure is the product of the result from the one-dimensional model and the azimuthal factor $C_n \Theta_n \exp[\mathrm{i}n\theta_x]$:

$$p(\mathbf{x},t) \propto A[\mathbf{x}; R, a_\infty, \omega, k, \lambda] \exp\left[\mathrm{i}\omega(t - |\mathbf{x}|/a_\infty)\right] \sum_{n=-\infty}^{\infty} C_n \Theta_n e^{\mathrm{i}n\theta_x}, \tag{6}$$

where the other factors that have been aggregated into A for compactness.

In order to make a meaningful assessment of the contribution of varying azimuthal extent, it is necessary to assume a model of the azimuthal extent. While a time and space-varying model would be the most representative, that level of complexity rapidly becomes analytically intractable. Therefore, a model that is independent of both t and y_1 will be used. A simple model for the azimuthal extent is a Gaussian with the scale parameter (β). As $\beta \rightarrow \infty$, the Gaussian models an axisymmetric source (i.e. $m = 0$) while small values for β model azimuthally confined sources.

Without loss of generality, the peak of the Gaussian can be placed at $\theta = 0$. The Fourier coefficients of the Gaussian are

$$\begin{aligned} C_n &= \frac{1}{2\pi} \int_{-\pi}^{\pi} e^{-\theta^2/\beta^2} e^{-\mathrm{i}n\theta} d\theta \\ &= \frac{\beta}{4\sqrt{\pi}} \left(\mathrm{erf}\left[\frac{\pi}{\beta} + \frac{\mathrm{i}n\beta}{2}\right] + \mathrm{erf}\left[\frac{\pi}{\beta} - \frac{\mathrm{i}n\beta}{2}\right] \right) \exp[-n^2\beta^2/4]. \end{aligned} \tag{7}$$

Since the Gaussian is a real even function, all the coefficients (C_n) are real and $C_n = C_{-n}$. In order to put the width of the Gaussian on a more physical footing, β is defined as

$$\beta \equiv \frac{\pi\, \delta\theta}{\sqrt{\ln[2]}}, \tag{8}$$

so that $\delta\theta$ is the fraction of the azimuth with an amplitude greater than 1/2. For values of $\delta\theta > 1$, the entire azimuth will have an amplitude greater than 1/2, so $\delta\theta$ loses its meaning. In order for a completely axisymmetric structure to be considered, however, $\delta\theta$ must be allowed to go to infinity. Therefore, values greater than one should be considered to observe the asymptotic behavior as the model limits to the axisymmetric case.

The properties of the Fourier coefficients of the Gaussian allow for additional simplification of the far-field pressure in eqn (6). For simplicity, the far-field azimuthal coordinate (θ_x) is set to zero at this time. Retaining θ_x complicates the subsequent expressions, but doesn't significantly impact the behaviors under discussion. The summation over the Fourier components can be separated into a real and imaginary portion,

$$\sum_{n=-\infty}^{\infty} C_n \Theta_n = M_{even} + \mathrm{i} M_{odd}, \tag{9}$$

where M_{even} & M_{odd} are the summations over the even and odd terms respectively. Incorporating this result into eqn (6) and retaining only the real portion, the far-field pressure is

$$p(\mathbf{x}, t) \propto A[\mathbf{x}; R, a_\infty, \omega, k, \lambda] \left\{ \cos\left[\omega(t - |\mathbf{x}|/a_\infty)\right] M_{even} - \sin\left[\omega(t - |\mathbf{x}|/a_\infty)\right] M_{odd} \right\}. \tag{10}$$

From eqn (10) it can be seen that the normalized acoustic power in the far-field is

$$W_p = \frac{1}{A^2 T} \int_0^T p^2 dt = \frac{1}{2} \left(M_{even}^2 + M_{odd}^2 \right), \tag{11}$$

where T is the period of the far-field signal and the power has been normalized by A^2 so that the quantity W_p is a dimensionless representation of the energy contribution from only the azimuthal factor. In order to numerically evaluate this result, values for St_D, M_a, and ϕ are required. Using values relevant to the experimental basis for this discussion (St_D = 0.2, M_a = 1, ϕ = 30°), Table 3 is computed for several azimuthal extents ($\delta\theta$). In addition to the acoustic power (W_p), Table 3 also contains the energy of the Gaussian (E) and the acoustic power normalized by the Gaussian energy. Since the Gaussian always has unit amplitude, its energy changes as the extent ($\delta\theta$) changes. It is therefore possible that the acoustic power could be simply scaling with the energy of the Gaussian. Normalizing the acoustic power by the Gaussian energy eliminates this source of ambiguity to focus on the essential quantity – the acoustic efficiency of the source.

The first thing to notice is that the radiating efficiency (W_p/E) increases with increasing $\delta\theta$ (i.e. the radiating efficiency of a source increases with increasing azimuthal extent). As $\delta\theta \to \infty$ (i.e. the extent limits to an axisymmetric source), the

radiating efficiency saturates indicating that sources which are approximately axisymmetric can be treated as axisymmetric when considering their radiation behavior.

Table 3: Radiated power versus azimuthal extent ($\delta\theta$) for St_D = 0.2, M_a =1, & ϕ = 30°.

$\delta\theta$	β	$E = C_n C_n$	W_p	W/E
0.01	0.038	7.53×10^{-3}	2.24×10^{-3}	0.297
0.1	0.377	7.53×10^{-2}	0.223	2.97
0.2	0.755	0.151	0.892	5.93
0.5	1.89	0.376	5.22	13.9
1	3.77	0.681	12.4	18.2
10	37.7	0.995	18.7	18.8

While not tabulated, there are additional behaviors of note with regard to varying the Strouhal number. For $\delta\theta \ll 1$, the acoustic power is independent of the Strouhal number. When $\delta\theta \geq 1$, only the zeroth order Fourier coefficient is significantly non-zero so the acoustic power behaves like a zeroth order Bessel function (i.e. J_0) when varying the Strouhal number. Obviously, the complete far-field pressure eqn (10) has many dependencies resulting in a complex behavior that cannot be easily described in words – and this is a very simplistic model. The preceding highlights a few of the relevant characteristics for the purpose of the present discussion.

The result of this azimuthal extent model provides a basis for some of the suppositions made regarding the varying responses to different modes of azimuthal excitation. Exciting the jet with higher order azimuthal modes restricts the azimuthal extent of the structures, which should create a corresponding restriction of the sources. Within the scope of this model, this result shows that these confined sources are less efficient radiators. If one imagines exciting azimuthal mode three as three independent sources each with an extent of $\delta\theta$ =0.1, the combined power would be 3 × 2.97 = 8.91 (where 2.97 came from the appropriate entry in Table 3). Thus, several azimuthally smaller sources are still weaker radiators than one axisymmetric source. As an alternative example, the acoustic power for a purely axisymmetric source using the same parameters as those used to generate Table 3 (St_D =0.2, M_a = 1, ϕ = 30°) is W_p = 18.8 while the acoustic power for a purely mode three source with the same parameters is $W_p = 8.14 \times 10^{-6}$. The disparity in this case is very much larger because of the use of a single simple harmonic as the model of the azimuthal extent. In reality, the decrease in radiating efficiency created by exciting mode three is probably somewhere between the two examples just discussed since a simple harmonic is an over-simplification and the neighboring structures in an $m_F = 3$ excited jet aren't actually independent.

If the azimuthal extent of a structure were to vary over the lifetime of a structure (as should be expected given the highly turbulent nature of the jet), the above provides a possible model for the inductive argument made at the end of §4. While it is possible to numerically model a source with time dependent Fourier coefficients, it is analytically intractable and the model already presented provides a sufficient basis for a discussion.

When a structure is first created (i.e. has small azimuthal extent), this model indicates that it is a relatively inefficient radiator. Under the right circumstances (i.e. structure is able to grow/merge to become significantly axisymmetric), this structure will experience a period of time during which it has a large azimuthal extent and high noise source energy that would result in a period of increased radiating efficiency and radiating power. This period of increased radiation would be a noise event. This allows for the uncoupling of the axial frequency (which should be directly related to the intermittence) from the event width (which the data show is a fraction of the intermittence) while still maintaining a close relationship between the two quantities through the governing dynamics of vortex evolution.

7. SUMMARY AND CONCLUSIONS

An experimental database from the Ohio State University Gas Dynamics and Turbulence Laboratory of far-field acoustic data from an excited subsonic ($M_j = 0.9$) jet at various temperatures (TTR = 1.0 – 2.5) was analyzed using the same process described in [9] (a previous work on unexcited subsonic jets based on data from NASA's AeroAcoustic Propulsion Laboratory) to explore how the characteristics of these noise events and their production are affected by excitation. Additionally, the known flow-field dynamics of the excited jet were used to inform the discussion of the noise event characteristics in relation to the flow-field. The jet was excited using an array of eight Localized Arc Filament Plasma Actuators (LAFPAs) spaced azimuthally around the nozzle exit. The excitation azimuthal modes and Strouhal numbers examined were $m_F = 0$, 1, & 3 and $St_{DF} = 0.09 – 3.0$, respectively. The basic characteristics of the signal analysis from this database matched those from the unexcited database [9]; this indicated that the dynamics being examined are general and not facility dependent. In addition to the experimental acoustic database, conclusions and observations from previous works using LAFPAs were leveraged to inform discussion of the statistical results and their relationship to the flow-field dynamics.

The results from the excited jet exposed several important characteristics that wouldn't have been discovered without the use of excitation. Analysis of the noise events revealed the existence of a resonance condition in the jet. When the jet is excited at a frequency matching the mean intermittence of the unexcited jet, large noise amplification can occur. This phenomenon is particularly pronounced when exciting the axisymmetric mode. When this occurs, nearly every large-scale structure produces a noise event. Conversely, noise reduction occurs when only a fraction of the large-scale structures produce noise events. The most substantial noise reduction occurs when the jet is excited with $m_F = 3$ and frequencies in the range $St_{DF} = 0.5 – 1.0$ depending on jet temperature. The other modes also produce noise reduction, but $m_F = 3$ (the highest simple azimuthal mode that could be excited by 8 LAFPAs) had the most pronounced effect.

Incorporating a previous work [61] on the hydrodynamic near-field in an excited jet, the behavior and interaction of the large-scale structures in relation to the noise event characteristics was discussed. This experiment also used a 2.54 cm diameter unheated

jet operated at $M_j = 0.9$ excited with the axisymmetric mode. The signature of the jet structures was measured by microphones placed in the hydrodynamic near-field region. It was found that the peak in the energy density of the large-scale structures corresponds reasonably well with the resonance condition found in the acoustic results. Further exploration of the excited jet near-field showed that, for excitation frequencies greater than $St_{DF} \approx 0.25$, the large-scale structures significantly interact with each other and this competition for flow energy inhibits the size and energy of the structures.

Leveraging the known dynamics of the excited jet flow-field, it was possible to use the current results to comment on the nature of jet noise production. Depending on the axial and azimuthal proximity of adjacent structures, initially separate structures can combine, work collaboratively to extract energy from the flow, or stifle each other's ability to extract energy. When the structures are able to consistently extract large amounts of flow energy, they produce strong noise events. When energy extraction is inhibited, noise production is reduced. Noise reduction through excitation is achieved by exciting the jet into a configuration that has reduced noise production while also inhibiting the naturally occurring structures.

Using a wave-packet model on a cylindrical surface, the impact of the azimuthal extent of a source was examined. By modeling the azimuthal extent as a Gaussian, it was possible to write down an analytical expression for the azimuthal radiating efficiency (i.e. the efficiency of a radiating source with respect to azimuthal extent). Using this expression it was shown that an axisymmetric structure is the most efficient radiator of sound (within the scope of the model). A structure covering only a fraction of the azimuth is less efficient and the efficiency increases monotonically with increasing azimuthal extent. It was proposed that a time varying azimuthal extent could partially decouple the axial frequency (i.e. the event intermittence) from the event width. This hypothesis provides a possible explanation for the close correlation found between these two time parameters in the results (both in this work and in [9]) despite the parameters being separated by a characteristic value of $\overline{\delta t} = 0.128\overline{\Delta T}$.

The results presented in this work suggest a process in which noise sources radiating to aft angles are competing for flow energy and that these noise sources are closely related to the large-scale structures. This and other recent works are revealing the existence of a wealth of new information on jet noise that can be accessed by the combined techniques of exciting the jet to control the dynamics of the turbulent structures and analyzing the noise production in terms of discrete events. While the present work is certainly not a solution to the problem of jet noise, it shows that there is plenty of relevant information waiting to be accessed using tools like these.

ACKNOWLEDGEMENTS

The support of this work by the Air Force of Office of Scientific Research (with Dr. John Schmisseur) and the NASA Glenn Research Center (with Drs. James Bridges and Clifford Brown) is greatly appreciated.

REFERENCES

1. Lighthill, M., "On Sound Generated Aerodynamically. I. General Theory," *Proceedings of the Royal Society of London*. Series A, 1952, Vol. 211, No. 1107, pp. 564-587.
2. Jordan, P. and Gervais, Y., "Subsonic jet aeroacoustics: associating experiment, modelling and simulation," *Experiments in Fluids*, 2008, Vol. 44, No. 1, pp. 1-21.
3. Tam, C. K. W., Golebiowski, M., and Seiner, J. M., "On the Two Components of Turbulent Mixing Noise from Supersonic Jets," *AIAA Paper 1996-1716*, 1996.
4. Viswanathan, K., "Scaling Laws and a Method for Identifying Components of Jet Noise," *AIAA Journal*, 2006, Vol. 44, No. 10, pp. 2274-2285.
5. Jordan, P., and Colonius, T., "Wave Packets and Turbulent Jet Noise," *Annual Review of Fluid Mechanics*, 2013, Vol. 45, pp. 173-195.
6. Cabana, M., Fortun, V., and Jordan, P., "Identifying the radiating core of Lighthill's source term," *Theoretical and Computational Fluid Dynamics*, 2008, Vol. 22, No. 2, pp. 87-106.
7. Kearney-Fischer, M., Sinha, A., and Samimy, M., "Time-Domain Analysis of Subsonic Jet Noise," *AIAA Paper 2012-1167*, 2012.
8. Kearney-Fischer, M., Sinha, A., and Samimy, M., "Time-Domain Analysis of Excited Subsonic Jet Noise," *AIAA Paper 2012-2209*, 2012.
9. Kearney-Fischer, M., Sinha, A., and Samimy, M., "The Intermittent Nature of Subsonic Jet Noise," *AIAA Journal*, 2013, Vol. 51, No. 5, pp. 1142-1155.
10. Morris, P. J., and Viswanathan, K., "Jet Noise," *Noise Sources in Turbulent Shear Flows: Fundamentals and Applications*, Ed. Camussi, R., Springer Verlag, 2013.
11. Samimy, M., Zaman, K. B. M. Q., and Reeder, M. F., "effect of Tabs on the Flow and Noise Field of an Axisymmetric Jet," *AIAA Journal*, 1993, Vol. 31, No. 4, pp. 609-619.
12. Zaman, K. B. M. Q., Reeder, M. F., and Samimy, M., "Control of an Axisymmetric Jet Using Vortex Generators," *Physics of Fluids*, 1994, Vol. 6, No. 2, pp. 778-793.
13. Kim, J. and Samimy, M., "Mixing Enhancement via Nozzle Trailing Edge Modifications in a High Speed Rectangular Jet," *Physics of Fluids*, 1999, Vol. 11, No. 9, pp. 2731-2742.
14. Saiyed, N. H., Mikkelsen, K. L., and Bridges, J. E., "Acoustics and Thrust of Quiet Separate-Flow High-Bypass-Ratio Nozzles," *AIAA Journal*, 2003, Vol. 41, No. 3, pp. 372-378.
15. Callender, B., Gutmark, E., and Martens, S., "Far-Field Acoustic Investigation into Chevron Nozzle Mechanisms and Trends," *AIAA Journal*, 2004, Vol. 43, No. 1, pp. 87-95.
16. Viswanathan, K., "Nozzle Shaping for Reduction of Jet Noise from Single Jets," *AIAA Journal*, 2005, Vol. 43, No. 5, pp. 1008-1022.

17. Crow, S. C. and Champagne, F. H., "Orderly Structure in Jet Turbulences," *Journal of Fluid Mechanics*, 1971, Vol. 48, No. 3, pp. 547-591.
18. Kibens, V., "Discrete Noise Spectrum Generated by an Acoustically Excited Jet," *AIAA Journal,* 1980, Vol. 18, No. 4, pp. 434-441.
19. Zaman, K. B. M. Q. and Hussain, A. K. M. F., "Vortex pairing in a circular jet under controlled excitation. Part 1. General jet response," *Journal of Fluid Mechanics,* 1980, Vol. 101, No. 3, pp. 449-491.
20. Zaman, K. B. M. Q. and Hussain, A. K. M. F., "Turbulence Suppression in Free Shear Flows by Controlled Excitation," *Journal of Fluid Mechanics*, 1981, Vol. 103, pp. 133-159.
21. Gutmark, E. and Ho, C. M., "Preferred Modes and the Spreading Rated of Jets," *Physics of Fluids*, 1983, Vol. 26, No. 10, pp. 2932-2938.
22. Ho, C. M. and Huerre, P., "Perturbed free shear layers," *Annual Review of Fluid Mechanics*, 1984, Vol. 16, pp. 365-424.
23. Cohen, J. and Wygnanski, I., "The evolution of instabilities in the axisymmetric jet. Part 1 the linear growth of disturbances near nozzle," *Journal of Fluid Mechanics*, 1987, Vol. 176, pp. 191-219.
24. Monkewitz, P., Bechert, D., Barsikow, B., and Lehmann, B., "Self-excited oscillations and mixing in a heated round jet," *Journal of Fluid Mechanics*, 1990, Vol. 213, pp. 611-639.
25. Lesshafft, L., Huerre, P., and Sagaut, P., "Aerodynamic Sound Generation by Global Modes in Hot Jets," *Journal of Fluid Mechanics*, 2010, Vol. 647, pp. 473-489.
26. Jendoubi, S. and Strykowski, P., "Absolute and Convective Instability of Axisymmetric Jets with External Flow," *Physics of Fluids*, 1994, Vol. 6, No. 9, pp. 3000-3009.
27. Michalke, A., "Survey on Jet Instability Theory," *Progress in Aerospace Sciences*, 1984, Vol. 21, pp. 159-199.
28. Samimy, M., Adamovich, I., Webb, B., Kastner, J., Hileman, J., Keshav, S., and Palm, P., "Development and characterization of plasma actuators for high-speed jet control," *Experiments in Fluids*, 2004, Vol. 37, No. 4, pp. 577-588.
29. Kim, J.-H., Nishihara, M., Adamovich, I., Samimy, M., Gorbatov, S., and Pliavaka, F., "Development of Localized Arc Filament RF Plasma Actuators for High-Speed and High Reynolds Number Flow Control," *Experiments in Fluids*, 2010, Vol. 49, No. 2, pp. 497-511.
30. Samimy, M., Kim, J., Kastner, J., Adamovich, I., and Utkin, Y., "Active Control of a Mach 0.9 Jet for Noise Mitigation Using Plasma Actuators," *AIAA Journal*, 2007, Vol. 45, No. 4, pp. 890-901.
31. Samimy, M., Kim, J.-H., Kastner, J., Adamovich, I., and Utkin, Y., "Active control of high-speed and high-Reynolds-number jets using plasma actuators," *Journal of Fluid Mechanics*, 2007, Vol. 578, pp. 305-330.

32. Kim, J.-H., Kastner, J., and Samimy, M., "Active Control of a High Reynolds Number Mach 0.9 Axisymmetric Jet," *AIAA Journal*, 2009, Vol. 47, No. 1, pp. 116-128.
33. Kearney-Fischer, M., Kim, J.-H., and Samimy, M., "Control of a high Reynolds number Mach 0.9 heated jet using plasma actuators," *Physics of Fluids*, 2009, Vol. 21, No. 9, pp. 095101.
34. Samimy, M., Kim, J.-H., Kearney-Fischer, M., and Sinha, A., "Acoustic and Flow Fields of an Excited High Reynolds Number Axisymmetric Supersonic Jet," *Journal of Fluid Mechanics*, 2010, Vol. 656, pp. 507-529.
35. Kearney-Fischer, M. and Samimy, M., "Noise Control of a High Reynolds Number Mach 1.3 Heated Jet Using Plasma Actuators," *AIAA Paper 2010-0013*, 2010.
36. Kearney-Fischer, M., Kim, J.-H., and Samimy, M., "Flow Control of a High Reynolds Number Mach 1.3 Heated Jet Using Plasma Actuators," *AIAA Paper 2010-4418*, 2010.
37. Kearney-Fischer, M., Kim, J.-H., and Samimy, M., "Noise Control of a High Reynolds Number High Speed Heated Jet Using Plasma Actuators," *International Journal of Aeroacoustics*, 2011, Vol. 10, No. 5-6, pp. 635-658.
38. Samimy, M., Kearney-Fischer, M., Kim, J.-H., and Sinha, A., "High Speed and High Reynolds Number Jet Control Using Arc Filament Plasma Actuators for Noise Mitigation and for Flow and Noise Diagnostics," *Journal of Propulsion and Power*, 2012, Vol. 28, No. 2, pp. 269-280.
39. Hileman, J., Thurow, B., Caraballo, E., and Samimy, M., "Large-scale structure evolution and sound emission in high-speed jets: real-time visualization with simultaneous acoustic measurements," *Journal of Fluid Mechanics*, 2005, Vol. 544, pp. 277-307.
40. Grassucci, D., Camussi, R., Kerherv, F., Jordan, P., and Grizzi, S., "Using Wavelet transforms and Linear Stochastic Estimation to study nearfield and turbulent velocity signatures in free jets," *AIAA Paper* 2010-3954, 2010.
41. Cavalieri, A. V., Jordan, P., Agarwal, A., and Gervais, Y., "Jittering wave-packet models for subsonic jet noise," *Journal of Sound and Vibration*, 2011, Vol. 330, No. 18-19, pp. 4474-4492.
42. Koenig, M., Cavalieri, A., Jordan, P., Delville, J., Gervais, Y., Papamoschou, D., Samimy, M., and Lele, S., "Farfield filtering and source imaging for the study of jet noise," *AIAA Paper* 2010-3779, 2010.
43. Guj, G., Carley, M., Camussi, R., and Ragni, A., "Acoustic Identification of coherent structures in a turbulent jet," *Journal of Sound and Vibration*, 2003, Vol. 259, No. 5, pp. 1037-1065.
44. Juve, D., Sunyach, M., and Comte-Bellot, G., "Intermittency of the Noise Emission in Subsonic Cold Jets," *Journal of Sound and Vibration*, 1980, Vol. 71, No. 3, pp. 319-332.

45. Lewalle, J., Low, K. R., and Glauser, M. N., "Properties of the far-field pressure signatures of individual jet noise sources," *International Journal of Aeroacoustics*, 2012, Vol. 11, No. 5-6, pp. 651-674.
46. Kastner, J., Kim, J.-H., and Samimy, M., "A study of the correlation of large-scale structure dynamics and far-field radiated noise in an excited Mach 0.9 jet," *International Journal of Aeroacoustics*, 2009, Vol. 8, No. 3, pp. 231-259.
47. Cavalieri, A. V. G., Jordan, P., Gervais, Y., Wei, M., and Freund, J. B., "Intermittent sound generation and its control in a free-shear flow," *Physics of Fluids*, 2010, Vol. 22, No. 11, pp. 115113.
48. Wei, M. and Freund, J. B., "A noise-controlled free shear flow," *Journal of Fluid Mechanics*, 2006, Vol. 546, pp. 123-152.
49. Kastner, J., Samimy, M., Hileman, J., and Freund, J. B., "Comparison of Noise Mechanisms in High and Low Reynolds Number High-Speed Jets," *AIAA Journal*, 2006, Vol. 44, No. 10, pp. 2251-2258.
50. Grizzi, S. and Camussi, R., "Wavelet analysis of near-field pressure fluctuations generated by a subsonic jet," *Journal of Fluid Mechanics*, 2012, Vol. 698, pp. 93-124.
51. Koenig, M., Cavalieri, A. V. G., Jordan, P., Delville, J., Gervais, Y., and Papamoschou, D., "Farfield filtering of subsonic jet noise: Mach and Temperature effects," *AIAA Paper 2011–2926*, 2011.
52. Koenig, M., Cavalieri, A. V. G., Jordan, P., and Gervais, Y., "Intermittency of the azimuthal components of the sound radiated by subsonic jets," *AIAA Paper 2011-2746*, 2011.
53. Low, K. R., Berger, Z. P., Lewalle, J., El-Hadidi, B., and Glauser, M. N., "Correlations and Wavelet Based Analysis of Near-Field and Far-Field Pressure of a Controlled High Speed Jet," 2011.
54. Kerechanin II, C. W., Samimy, M., and Kim, J. H., "effects of Nozzle Trailing Edges on Acoustic Field of Supersonic Rectangular Jet," *AIAA Journal*, 2001, Vol. 39, No. 6, pp. 1065- 1070.
55. Kearney-Fischer, M., Kim, J.-H., and Samimy, M., "A Study of Mach Wave Radiation Using Active Control," *Journal of Fluid Mechanics*, 2011, Vol. 681, pp. 261-292.
56. Suzuki, T. and Colonius, T., "Instability waves in a subsonic round jet detected using a near-field phased microphone array," *Journal of Fluid Mechanics*, 2006, Vol. 565, pp. 197-226.
57. Hall, A. M. and Glauser, M. N., "An experimental analysis of the modal characteristics intrinsic to both the heated and cold jet," *AIAA Paper 2009-1238*, 2009.
58. Kastner, J., "Far-Field Radiated Noise Mechanisms in High Reynolds Number and High-Speed Jets," Ohio State University, PhD Thesis, 2007.

59. Crighton, D. G. and Huerre, P., "Shear-layer pressure fluctuations and superdirective acoustic sources," *Journal of Fluid Mechanics*, 1990, Vol. 220, pp. 355-368.
60. Hall, J. W., Pinier, J., Hall, A., and Glauser, M., "Two-point correlations of the near and far-field pressure in a transonic jet," *ASME Paper FEDSM2006-98458*, 2006.
61. Sinha, A., Alkandry, H., Kearney-Fischer, M., Samimy, M., and Colonius, T., "The impulse response of a high-speed jet forced with localized arc filament plasma actuators," *Physics of Fluids*, 2012, Vol. 24, No. 12, pp. 125104.
62. Gaitonde, D. V., "Analysis of the Near Field in a Plasma-Actuator-Controlled Supersonic Jet," *Journal of Propulsion and Power*, 2012, Vol. 28, No. 2, pp. 281-292.
63. Cavalieri, A. V. G., Jordan, P., Colonius, T., and Gervais, Y., "Axisymmetric superdirectivity in subsonic jets," *Journal of Fluid Mechanics*, 2012, Vol. 704, pp. 388-420.